Incorporating Mouse Genome
Mammalian Genome
Genes and Phenotypes

# Comparative genomics of xenobiotic metabolism: a porcine-human PXR gene comparison

**Callie B. Pollock, Margarita B. Rogatcheva, Lawrence B. Schook**

Department of Animal Sciences, University of Illinois at Urbana-Champaign, Urbana, Illinois 61801, USA

*Received: 4 December 2006 / Accepted: 6 February 2007*

### Abstract

The pregnane X receptor (PXR) plays a crucial role in xenobiotic and drug metabolism, being the major transcriptional regulator of cytochrome P-450 monooxygenase 3A4, which metabolizes more than 50% of all clinically used drugs. Recent pharmacodynamic studies have shown that the mouse is not an ideal model for predicting human clinical drug study outcomes. Therefore, we characterized the porcine *PXR* (*pPXR*) gene to evaluate the utility of the pig as an alternate preclinical animal model. The complete sequence of *pPXR* mRNA and 11 kb of genomic sequence were obtained. Similar to the human *PXR* gene, the *pPXR* gene revealed multiple splice variants in the ligand-binding domain. All *pPXR* splice variants (SV) were porcine-specific. The *pPXR* mRNAs varied in 3′-UTR length due to differential termination and specific deletions. Northern blot analyses identified high levels of *pPXR* mRNA expression in the liver, small intestine, heart, kidney, and colon. RT-PCR amplification detected lower levels of *pPXR* expression in multiple tissues. Ninety-three pigs representing eight breeds were analyzed for single nucleotide polymorphisms (SNPs). Only one nonsynonymous SNP (S178L) was found in the *pPXR* ligand-binding domain. This characterization of the *pPXR* gene contributes to the development of a porcine model for human drug metabolic studies.

*Present address: Northwestern University Feinberg School of Medicine, Evanston, Illinois, USA
Correspondence to: Lawrence B. Schook, Department of Animal Sciences, University of Illinois at Urbana-Champaign, 1201 W. Gregory Dr., Edward R. Madigan Laboratory 382 Urbana, IL 61801, USA; E-mail: schook@uiuc.edu

### Introduction

The pregnane X receptor (PXR) plays a critical role in mammalian xenobiotic metabolism. PXR is a nuclear hormone receptor that has been shown to transcriptionally regulate cytochrome P4503A4 (CYP3A4) (Bertilsson et al. 1998; Kliewer et al. 1998). CYP3A4 is responsible for catabolism of over 50% of all pharmaceutical drugs currently in clinical use (Maurel 1996) and PXR plays such a significant role in the regulation of CYP3A4. Thus, examining this gene and defining genetic polymorphisms is important to our understanding of individual responses towards drugs. Consequently, many studies have focused on characterization of the human PXR.

The human *PXR* (*hPXR*) gene contains nine exons with an open reading frame (ORF) spanning exons 2–9, producing a 434-amino-acid peptide (Zhang et al. 2001). The *hPXR* contains two major domains, a DNA-binding domain and a ligand-binding domain. The *hPXR* ligand-binding domain binds to a diverse array of molecules, including endogenous compounds like progesterone and bile acids (Kliewer et al. 1998), exogenous chemicals including drugs like rifampin (Blumberg et al. 1998), or immunosuppressive agents (Maurel 1996). The hPXR is ligand activated by xenobiotics or endobiotics and then binds as a heterodimer with the retinoid-X receptor to the promoter region and activates CYP3A4 transcription (Handschin and Meyer 2003). Further investigation of the *hPXR* has focused on defining splice variants (SVs) and tissue expression to explore additional functional roles and ligand-binding abilities of hPXR (Lamba et al. 2004). In addition, single nucleotide polymorphisms (SNP) of *hPXR* have been explored as a means of altering CYP3A4 induction (Zhang et al. 2001). Studies such as these revealed a new layer of complexity for the

 DOI: 10.1007/s00335-007-9007-7 • Volume 18, 210–219 (2007) 

*hPXR* gene by describing how the composition of transcribed and translated products varies with factors such as drug exposure (Pascussi et al. 2000) and disease state (Langmann et al. 2004) and represents individual and population-specific variants (Hustert et al. 2001; Zhang et al. 2001; Koyano et al. 2004; Lim et al. 2005).

Less is known about the *PXR* orthologs in potential animal models. It is important to identify suitable animal models for pharmacogenomic drug studies because it is often unethical to use human participants. Therefore, additional data focusing on the *PXR* of common animal models, in particular, the pig, should be generated to aid in the identification of relevant preclinical models. While the mouse is a common choice in the development of animal models, it has recently been shown that it may not be ideal for use in drug studies because protein sequence divergence results in drugs being metabolized differently in mice than by humans (Xie et al. 2000). Past comparisons between the human and the mouse PXR have shown that single amino acid differences can change PXR activity (Ostberg et al. 2002). Furthermore, transgenic mice with introduced human residues in four locations (R203, P205, Q404, and Q407) functioned like the human PXR when binding SR12813 (Watkins et al. 2001). The porcine PXR has been shown to have a higher similarity to human PXR than mouse PXR (87% vs. 77% identity) and contains the human residues at these four locations (Moore et al. 2002). This suggests that the pig could act as a useful pharmacogenomic model in addition to the recently developed humanized mouse model (Ma et al. 2007). This study provides an in-depth characterization of the *pPXR* gene, including an analysis of SVs, gene expression profiles, and SNPs analyses.

## Materials and methods

***Sequencing of pPXR gene.*** The precise chromosomal location of the *hPXR* was obtained (120982021–121020022 bp on HSA3) using the latest human draft (build 36.2) on the NCBI browser (http://www.ncbi.nih.gov). The *hPXR* chromosomal information was then used to search for the porcine orthologous (*pPXR*) sequences contained in BACs of the CHORI-242 porcine BAC library (http://www.bacpac.chori.org/porcine242.htm) using an *in silico* tool (http://www.sanger.ac.uk/Projects/S_scrofa/mapping.stml). The BACs that were predicted to contain *pPXR* were further verified by PCR amplification of two fragments from the 3′ and 5′ ends of *pPXR* coding region using primer pairs located in exon 2 (5′-AGCTGGAGGTGAGACC TGAA-3′, 5′-CTCATCTGCATTGGTGGTGG-3′) and in exon 9 (5′-CCTGAAGATCATGGCTATGC-3′, 5′-GTGTATGTCCTGGATTCGCA-3′), respectively. Primers pairs were derived from the *pPXR* cDNA sequence (GenBank accession No. AB214980), where the exon–intron boundaries were preliminarily determined by comparing *pPXR* cDNA (GenBank accession No. AB214980) with human sequence data (GenBank accession No. AF364606).

The BAC containing *pPXR* was isolated with a NucleoBond plasmid purification kit (BD Biosceinces, Palo Alto, CA). Overlapping fragments, covering the genomic region from exon 2 to exon 9, were amplified from BAC DNA using primers (Table 1) designed from *pPXR* cDNA sequences (GenBank accession No. AB214980) based on the determined exon–intron borders. PCR fragments were purified with the QIAquick PCR Purification Kit (Qiagen, Valencia, CA) and bidirectionally sequenced using the ABI Prism® BigDye™ Cycle Sequencing Kit (version 3.1) (Applied Biosystems, Foster City, CA). All sequencing reactions were analyzed on an ABI 3730 DNA capillary sequencer (Applied Biosystems). The DNA regions not adequately covered by the first round of sequencing were cloned into the pCR®2.1-TOPO® vector (Invitrogen, Carlsbad, CA) and sequenced with nested primers designed to bridge sequence gaps. To determine the intronic sequence flanking the 3′ end of exon 2 and explore exon 9, primer walking and direct sequencing from the BAC was employed. Genomic organization of the *pPXR* was determined by the alignment of the obtained DNA fragments with cDNA sequences, and by comparative analysis with the *hPXR* sequences using the Vector NTI Suite 9 program. The obtained genomic sequence was deposited in GenBank with accession number DQ531715.

***RNA extraction and cDNA analysis.*** Total RNA was extracted from the following tissues of a Duroc × Berkshire pig breed $F_1$ cross: brain, heart, thymus, lung, trachea, liver, spleen, kidney, adrenal gland, thyroid, stomach, intestine, colon, mesenteric and mandibular lymph nodes, uterus, ovary, testis, muscle, skin, bone marrow, spinal cord, and fat. Extraction was accomplished using a Tryzol reagent (Invitrogen, Carlsbad, CA) according to the manufacturer's protocol. To remove genomic DNA contamination, mRNA samples were treated with DNaseI (Qiagen, Valencia, CA) and purified with the RNeasy Kit (Qiagen). Samples were reverse transcribed with oligo(dT)12–18 and random primers (Stratagene, La Jolla, CA) and Superscript II (H+) (Gibco-BRL, Gaithersburg, MD) using the manufac-

**Table 1. Primers used in PXR characterization**

| *Primer name* | *Exon/intron location* | *Base pair location* | *Sequence* | *Fragment size* |
|---|---|---|---|---|
| **Primers for BAC/mRNA sequencing** | | | | |
| PXRA2-3f | exon 2 | 707 | 5′-GCTGACCTCATGCAATGCAA-3′ | 2749 |
| PXRA2-3r | exon 3 | 3,456 | 5′-CTTCTTCATGCCGCTCTCCA-3′ | |
| PXRB3-4f | exon 3 | 3,379 | 5′-TGCGAGATCACCCGGAAGAC-3′ | 1479 |
| PXRB3-4r | exon 4 | 4,858 | 5′-CAGTGAGACCCTTGGCTCCT-3′ | |
| PXRC4-5f | exon 4 | 4,803 | 5′-GAGGAAGAAACGAGAACAGA-3′ | 1363 |
| PXRC4-5r | exon 5 | 6,166 | 5′-AGTAGGAGATGACTTTGGCA-3′ | |
| PXRD5-6f | exon 5 | 5,909 | 5′-GCAGTAGCCTCGAGATTCCA-3′ | 2388 |
| PXRD5-6r | exon 5 | 8,297 | 5′-GTCTCTGCGTTGAACACCGT-3′ | |
| PXRF6-8f | exon 6 | 8,208 | 5′-CTTGCCCATTGAGGACCAGA-3′ | 868 |
| PXRF6-8r | exon 8 | 9,076 | 5′-CGATGTAGGCCTTCAGGGTA-3′ | |
| PXRG8-9f | exon 8 | 9,033 | 5′-CCAGCTGCAGGAGAGGTTTG-3′ | 1261 |
| PXRG8-9r | exon 9 | 10,294 | 5′-GCGGAGCTCAGTGAGCATAG-3′ | |
| PXRin2-ex3F | intron 2 | 1,306 | 5′-GCCTCTGCCAATTTCCTGCT-3′ | 2152 |
| PXRin2-ex3R | exon 3 | 3,458 | 5′-TCCTTCTTCATGCCGCTCTC-3′ | |
| PXR5-6intf | intron 5 | 6,574 | 5′-CGAGGAGTTGGCAGGAAAGG-3′ | 1027 |
| PXR5-6intr | intron 5 | 7,601 | 5′-ATACCAGAGGCAGCGGCTGT-3′ | |
| PXR1600f | intron 2 | 1,960 | 5′-GCTACTAGCACGCTGATAGA-3′ | 847 |
| PXR1600r | intron 2 | 2,807 | 5′-CTCACTAGACAAAGGCTTCC-3′ | |
| PXR3200f | intron 3 | 3,624 | 5′-TTGCGGTTCAGGCGTTGTCT-3′ | 663 |
| PXR3200r | intron 3 | 4,287 | 5′-CCCAAATCTCCAGGTCTCCA-3′ | |
| PXR6600f | intron 5 | 7,149 | 5′-ACCCAGGATTTACCACCAGA-3′ | 621 |
| PXR6600r | intron 5 | 7,770 | 5′-CTCCTAAAGGGCTTTCCAGA-3′ | |
| PXRseq2 | exon 2 | 772 | 5′-CTCATCTGCATTGGTGGTGG-3′ | [a] |
| PXRseq9 | exon 9 | 10,280 | 5′-CCTGAAGATCATGGCTATGC-3′ | [a] |
| PXRex3f | intron 2 | 3,152 | 5′-AGCCCAGCACCAACAGAAGT-3′ | 337 |
| PXRex3r | intron 3 | 3,489 | 5′-CACGCCTGTCCATGTCGTAT-3′ | |
| PXRex4f | intron 3 | 4,519 | 5′-CTCAAGCCCAGTGCCTTTAG-3′ | 534 |
| PXRex4r | intron 4 | 5,053 | 5′-GGTGATGCTTCTGTGCTGGT-3′ | |
| PXRex5bf | intron 4 | 5,793 | 5′-GTGTGGCTGTGTGGGTGTGT-3 | 518 |
| PXRex5br | intron 5 | 6,311 | 5′-CAGGTGCCCTGGAGATAGAG-3′ | |
| PXRex6-7f | intron 5 | 8,000 | 5′-AGGTGGCAGAGAGGAGGAAT-3′ | 868 |
| PXRex6-7r | intron 7 | 8,868 | 5′-CTAAGAGGGCTTGGCATCAG-3′ | |
| PXRex8f | intron 7 | 8,836 | 5′-TAGGGTTGGAGGGCTGATGC-3′ | 294 |
| PXRex8r | intron 8 | 9,130 | 5′-TCACACCCTCCCTGCTTGCT-3′ | |
| PXRex2f | intron 1 | 474 | 5′-AATGTCCTGGTCACACCTCT-3′ | 645 |
| PXRex2r | intron 2 | 1,119 | 5′-TTCTGTGTAGGCCTCTCTTG-3′ | |
| PXRex9f | intron 8 | 10,060 | 5′-CCAGCTATTCTGCACCTGTT-3′ | 454 |
| PXRex9r | exon 9 | 10,514 | 5′-AGTAATGCTAGCCAGCCATC-3′ | |

[a]Primers not utilized to amplify fragments but rather used for direct BAC sequencing.

turer's protocol. The 3′ and 5′ RACE of total liver RNA was completed using the FirstChoice RLM RACE kit (Ambion, Austin, TX). The first round of 5′-RACE PCR included an initial enzyme activation at 95°C for 15 min, followed by 35 cycles of 95°C for 30 sec, 55°C for 30 sec, and 72°C for 2 min; then 72°C for 7 min. A second PCR round was performed using a nested *pPXR*-specific primer (5′-CTCATC TGCATTGGTGGTGG-3′) and a primer provided with the kit. PCR conditions were identical to the first round but the annealing temperature was raised by 2°C. The first round of 3′-RACE PCR was at 95°C for 15 min; 35 cycles at 95°C for 30 sec, 58°C for 30 sec, and 72°C for 4 min; then 72°C for 7 min. Similar to the 5′ RACE, a second round of amplification was performed using a nested *pPXR*-specific primer (5′-CCAGCTGCAGGAGAGGTTTG-3′) and the annealing temperature was raised by 2°C. The 3′- and 5′-RACE products were cloned into the pCR®2.1-TOPO® vector system (Invitrogen, Carlsbad, CA) and sequenced. Multiple primer pair sets (Table 1) were used to visualize *pPXR* mRNA SVs by amplifying cDNA fragments containing exons 2–9, exons 2–6, exons 5–9, exons 2–4, and exons 4–6. The resulting PCR fragments were cloned into the pCR®2.1-TOPO® vector and sequenced. The sequences of *pPXR* mRNA variants were deposited in GenBank with accession numbers DQ531716, DQ531717, DQ531718, DQ531719, DQ531720, and DQ531721.

***Tissue expression.*** The *PXR* gene expression pattern in eight tissues (heart, kidney, colon, brain, adrenal gland, liver, small intestine, and stomach) was analyzed by Northern blot hybridization. Twenty micrograms of total RNA were separated on a 1% agarose gel and blotted onto a Brightstar membrane (Ambion, Austin, TX). Blotting, washing, and hybridization were done with the Northern Max-Gly kit (Ambion) according to the manufacturer's protocol. A 1.2-kb fragment of *pPXR* cDNA was amplified with PXRA2-3f and PXRG8-9r primers (Table 1), labeled with the Megaprime DNA labeling system (Amersham Biosciences, England), and used as a hybridization probe. *PXR* expression in the above 8 tissues and in an additional 15 (thymus, lung, trachea, spleen, thyroid, mesenteric and mandibular lymph nodes, uterus, ovary, testis, muscle, skin, bone marrow, spinal cord, and fat) were further analyzed by PCR amplification (35 cyles) using exon-specific primers pairs: PXRA2-3f and PXRG8-9r (amplifies exons 2–9), PXRD5-6f and PXRG8-9r (amplifies exons 5–9) (Table 1). Beta-actin was used as a positive control to ensure the equal amount of cDNA template used for PCR amplifications.

***Single nucleotide polymorphism (SNP) identification.*** SNPs in the porcine *PXR* gene were detected using a direct sequencing approach of the *PXR* coding region of 93 unrelated pigs (no shared grandparents) with 8–12 individuals representing individual breeds. Breeds representing diverse phenotypes used in pork production and biomedical research included Hanford, Sinclair, Yucatan, Duroc, Pietrain, Hampshire, Yorkshire, and the Large White. Primers were designed from intronic regions flanking coding exons and from 3′ UTR on exon 9 of *pPXR* (Table 1). PCR fragments were amplified from DNA extracted from peripheral blood cells. PCR amplicons were purified using a Qiagen MinElute 96 UF PCR Purification kit (Qiagen, Valencia, CA) and bidirectionally sequenced using the same amplification primers. Resulting sequences were aligned and analyzed for SNPs with Seqencher software (version 4.1, Gene Codes Corporation, Ann Arbor, MI).

## Results

***Characterization of the porcine PXR gene.*** To characterize the *pPXR* gene, the genomic region spanning the entire ORF of the *pPXR* gene was sequenced from a single BAC (35F02) isolated from the porcine CHORI-242 BAC library. Six overlapping PCR fragments, covering the exon 2 to exon 9 region, were bidirectionally sequenced and assembled into a contiguous sequence spanning 10,997 bp (DQ531715). The DNA sequence of the *pPXR* genomic region together with the *pPXR* cDNA sequence permitted the definition of the *pPXR* gene exon–intron boundaries. The comparison to the *hPXR* gene shows that the length of exons and splicing site positions was analogous in both species (Fig. 1). Similar to the *hPXR* gene, the ORF of the *pPXR* gene spanned the region from exons 2 to exon 9 producing a 421-amino-acid peptide. This predicted *pPXR* peptide is comparable in length to the characterized 434-amino-acid *hPXR* peptide. Size differences were due to an additional 14 amino acids in the N-terminus of *hPXR* before the translational start of *pPXR* (NP003880). The inferred porcine protein sequence showed 85% sequence identity and 91% similarity with the human protein.

Previous research has demonstrated that the *hPXR* gene exhibits a number of sequence variants in the 5′ UTR resulting from both alternative splicing of leader exons and different transcriptional start sites (Kurose et al. 2005). To examine potential sequence variants in *pPXR* untranslated regions and to generate a complete sequence of the *pPXR* mRNA, 3′ and 5′ RACE were used. Only a single 5′ UTR of 223 bp was detected among *pPXR* liver transcripts. Comparison of the *pPXR* exon 1 (152 bp) and various 5′-UTR variants of *hPXR* revealed that *pPXR* exon 1 is similar to the 3′ end of *hPXR* exon 1a (548 bp) with 62% identity. Exon 1a of *hPXR* has several differential transcriptional starts (Kurose et al. 2005). Only the single transcription start was detected in *pPXR*, but the alternative 49-bp upstream start site was observed in the *pPXR* cDNA sequence previously deposited in GenBank (AB214980), providing evidence for differential *pPXR* transcriptional start sites. Thus, the porcine transcripts are analogs of the most abundant human splice variant PXR-1 (SXR or hPAR-1) (AF364606).

The assembled *pPXR* mRNA spanned 2496 bp (DQ531716). Northern blot hybridization of total porcine mRNA with a *pPXR* probe detected two major mRNA species (2.5 kb and 3.2 kb bands) (Fig. 2), where the 2.5-kb band corresponds to the *pPXR* mRNA reported in this and other studies (AB214980). A larger (3.2 kb) band could potentially represent a *pPXR* transcript(s) with a longer 5′ or 3′ UTR. While a number of 3′ UTRs were obtained by 3′ RACE and sequenced, none accounted for the longer 3.2-kb product identified by the Northern blot analysis. Instead, four additional sequence variants with shorter *pPXR* mRNA 3′ UTRs were detected. Interestingly, the length polymorphism of these 3′ UTRs was not only due to differential termination of mRNA, but mainly due to specific deletions within the 3′ UTRs (Fig. 3).

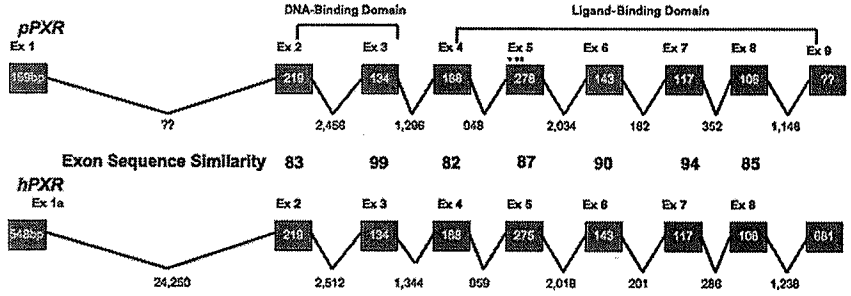


**Fig. 1.** Pig–human *PXR* gene comparison: schematic representation of human and porcine *PXR* genomic regions. Human sequence information from GenBank (AF364606). The *pPXR* genomic sequence was obtained by sequencing CHORI-242 BAC 35F2. Gray boxes represent exons with the exon size (bp) shown within each box. Intron size (bp) is listed between the exons. Asterisk marks denote SNP locations at 727, 756, and 760 bp (DQ531716).

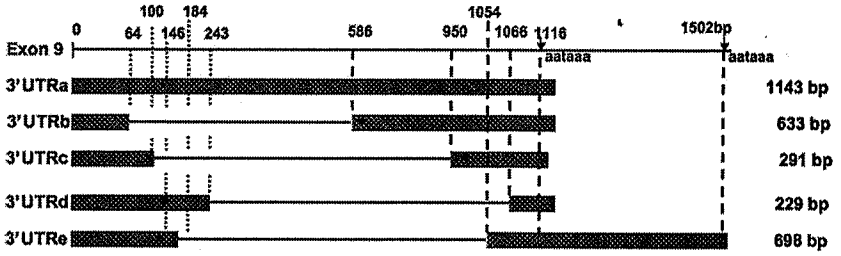


**Fig. 2.** Sequence variants of 3′ region (exon 9) in *pPXR* transcripts. The scale is matched to wild-type exon 9. The length of exon 9 in each variant is provided next to the variant. The asterisk indicates the stop codon. Deletions within exon 9 are marked in corresponding bp position on wild-type exon 9. Two arrows represent polyA termination signal sites.

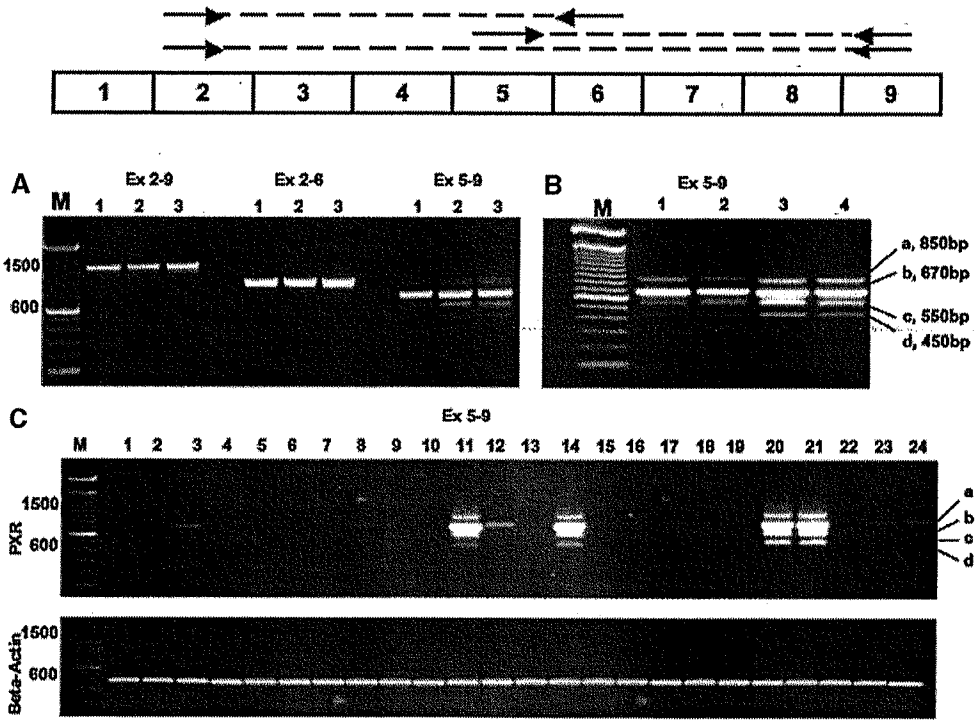


**Fig. 3.** Porcine *PXR* splice variant detection. (**A**) RT-PCR to amplify exon 2–9, exon 2–6, and exon 5–9 regions (depicted schematically in the top panel) was used to detect porcine splice variants in cDNA samples from (1) liver, (2) small intestine, and (3) colon. A 100-bp marker (Invitrogen, Carlsbad, CA) is indicated as M. (**B**) Exons 5–9 were PCR amplified yielding four distinct fragments: (1) liver, (2) kidney, (3) small intestine, and (4) colon. Major porcine variants are identified: (a) ssPXR.2, (b) ssPXR.1, (c) ssPXR.3 and/or ssPXR.5, (d) ssPXR.4 and/or ssPXR.6. (**C**) Exons 5–9 were amplified from a large sample of pig tissues to show relative abundance: (1) skin, (2) fat, (3) adrenal gland, (4) spinal cord, (5) muscle, (6) mandibular lymph node, (7) thyroid, (8) thymus, (9) trachea, (10) stomach, (11) liver, (12) heart, (13) bone marrow, (14) kidney, (15) ovary, (16) bladder, (17) lung, (18) spleen, (19) testicle, (20) small intestine, (21) colon, (22) brain, (23) uterus, (24) mesenchymal lymph nodes. The major porcine variants are labeled as was described in (**B**). PCR amplification of *β*-actin was used as a positive loading and amplification control.

***Characterization of pPXR splice variants.*** Alternatively spliced transcripts are common among nuclear receptors and have been previously observed in the *hPXR* (Fukuen et al. 2002). Thus, the *pPXR* gene was also screened for transcript variants. Three sets of PCR primers allowed the detection and clear visualization of multiple *pPXR* transcripts (Fig. 4). The first set of primers completely amplified the coding region from exon 2 to exon 9. A fragment with an expected length of 1.17 kb was obtained along with additional fragments of multiple divergent sizes. To resolve fragments of similar sizes, the same templates were used to amplify shorter fragments covering the exon 2–exon 6 or exon 5–exon 9 region (Fig. 4A). Within the exon 2–6 region only the expected PCR fragment of 856 bp was amplified. However, in the exon 5–9 region, four distinct fragments were observed. These included the expected and most abundant fragment of 670 bp and three additional fragments of approximately 450 bp, 550 bp, and 850 bp (Fig. 4B).

The four detected fragments consisted of six sequence variants which were 853, 670, 528, 536, 422, and 411 bp long. In addition to the predicted and most abundant wild-type mRNA isoform (ssPXR.1, DQ531717), five novel porcine variants, designated ssPXR.2 through ssPXR.6 (DQ531716, DQ531718, DQ531719, DQ531720, DQ53172), were detected. These variants resulted from the alternative splicing of exons 6, 7, and 8 and novel exon 6a (Fig. 5). The wild-type *pPXR* mRNA was translated into a 421-amino-acid peptide, whereas the early termination was predicted in the other three SV *pPXR* transcripts. The ssPXR.2 variant retains the complete intron 6 (182 bp) that was designated the novel "exon 6a." This leads to a predicted frameshift and truncated protein of 371 amino acids. The ssPXR.3 variant has an excised exon 6 (144 bp), producing a truncated putative peptide of 275 amino acids (aa). The ssPXR.4 variant excised both exon 6 and exon 8, leading to the same early termination of translation after 275 aa, as in the ssPXR.3. The ssPXR.5 variant excised exon 6 but retained 17 bp of the 3′ end of exon 6a observed in ssPXR.2, thus creating a putative peptide that was 42 aa shorter than the wild-type peptide. The ssPXR.6 variant spliced out both exons 5 and 7 and created a predicted truncated peptide of 298 aa.

All the detected *pPXR* mRNA variants were porcine-specific. The porcine transcriptional splicing involved exons 6, 6a, 7, and 8, whereas in humans major splicing events involve only exon 2 and exon 5. To search for "human-specific" variants, additional screening of the *pPXR* gene for alternation in porcine exon 2 and exon 5 (Fig. 5) was conducted.

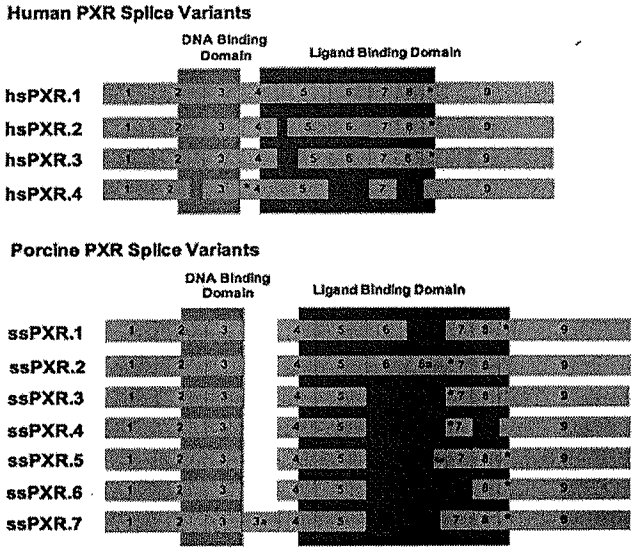


**Fig. 4.** Major human and porcine *PXR* splice variants. The *hPXR* variants are presented as described by Lamba et al. (2004). Exons are designated by boxes and the translational initiation site is demarcated with a flagged arrow above exon 2. The stop codon is represented with an asterisk and the approximate domain sites are highlighted with gray boxes. The hsPXR.1 and ssPXR.1 variants represent the respective "wild-type" transcripts of the human and pig.

The short fragments of *pPXR* from exon 2 to exon 4 and from exon 4 to exon 6 were PCR amplified from pig liver cDNA. The exon 4–6 amplification revealed no fragment length polymorphisms, whereas three faint variant fragments, all within 100 bp of the predicted fragment length, were detected within the exon 2–4 region. SVs observed in less than 5% of total transcripts often represent transcriptional errors (Kan et al. 2002). Thus, to determine if these low abundant transcripts were biologically relevant, the PCR amplicons of exons 2–4 were cloned and 50 independent isolates were sequenced and analyzed. Through this screening, only a single clone was found to be a new splice variant, ssPXR.7, which contained a 51-bp intronic insertion following exon 3. The ssPXR.7 variant does not correspond to any predicted or observed *hPXR* SVs. Because of its low abundance, this splice variant most likely represents a transcriptional error. In summary, none of the major SVs expressed by the *pPXR* gene corresponded

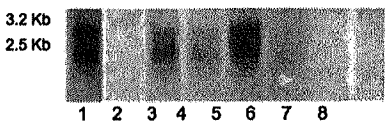


**Fig. 5.** Northern blot analysis of *pPXR* expression in eight tissues: (1) small intestine, (2) brain, (3) heart, (4) kidney, (5)liver, (6) colon, (7) stomach, and (8) adrenal gland. Two major transcript sizes are detected: 2.5 kb and 3.2 kb.

to the *hPXR* SVs, though minor human-like variants could remain undetectable.

In addition, we identified regions of high sequence conservation between human and porcine *PXR* genes using an exon–exon comparison. The most conserved exon (with a 99% sequence identity) is exon 3, which encodes the DNA-binding domain and is not spliced in either human or pig *PXR* (Fig. 1). The exons contributing to the ligand-binding domain (exons 4–8) and exon 2 has a range of 82%–94% sequence identities and each undergoes alternative splicing in one or another species.

To examine the relative abundance of the identified variants, PCR analysis of the exon 5 to exon 9 region was performed on an extended set of porcine tissues (brain, heart, thymus, lung, trachea, liver, spleen, adrenal gland, thyroid, stomach, mesenteric and mandibular lymph nodes, uterus, ovary, testis, muscle, skin, bone marrow, spinal cord, and fat). In the tissues with high total *pPXR* expression, each of the four fragments were highly represented indicating intensive alternative splicing of *pPXR* mRNA. The tissue with low abundances had one or several variant transcripts prevalent. No additional variants were detected.

***Tissue expression of PXR.*** To expand the characterization of *PXR* expression, tissue expression profiles were conducted using both Northern blot analysis and RT-PCR. Eight diverse tissues were analyzed by Northern blot (heart, kidney, colon, brain, adrenal, liver, small intestine, and stomach). Of these tissues, the liver and small intestine displayed the greatest level of expression with the heart, kidney, and colon tissues also displaying less abundant transcripts (Fig. 2). Expression of the porcine *PXR* gene was then verified by the PCR amplification of exons 5–9 with an extended set of porcine tissues (Fig. 4C). In addition to the already detected tissues with the high expression of *pPXR* gene (such as kidney, liver, small intestine, and colon), minor expression was observed in the adrenal gland, mandibular lymph node, thymus, ovary, uterus, trachea, bladder, spleen, and mesenchymal lymph node.

***Single nucleotide polymorphisms (SNPs).*** To address sequence variability, the *PXR* coding region, composed of eight exons (2–9), was amplified from the genomic DNA of 93 unrelated pigs representing eight breeds (Hanford, Sinclair, Yucatan, Duroc, Pietrain, Hampshire, Yorkshire, and Large White). Three SNPs were identified and located in exon 5; they comprise the ligand-binding domain, as is noted on Fig. 1. Two SNPs that represented synonymous changes were detected at 727 and 760 bp (DQ531716) or codon 169 and 180, respectively. The only nonsynonymous polymorphism identified involved a thymine/cytosine substitution at 756 bp (DQ531716) leading to a serine-to-leucine switch at codon 178. This represents a significant change involving the substitution of a polar- with a nonpolar-charged amino acid. To determine the frequency of the thymine/cytosine point mutation, the generated sequence information was examined on a breed-to-breed basis (Table 2). It was determined that the Hanford, Yucatan, Duroc, Pietrain, Yorkshire, and Large White breeds contained only the cytosine nucleotide in the S178L codon and thus were homozygous for the cytosine nucleotide (allele frequency of 1). The Sinclair and Hampshire breeds contained both cytosine and thymine alleles. Within the Sinclair population, the allele frequency for thymine was 0.125, whereas the Hampshire breed has an adenine allele frequency of 0.825 (Table 2).

**Table 2. PXR S178L nucleotide prevalence among pig breeds**

| | *Allele frequency* | |
|---|---|---|
| *Breed (No. of pigs)* | *Cytosine* | *Thymine* |
| Yucatan (9) | 1 | 0 |
| Duroc (12) | 1 | 0 |
| Pietrain (12) | 1 | 0 |
| Large White (12) | 1 | 0 |
| Hanford (12) | 1 | 0 |
| Yorkshire (12) | 1 | 0 |
| Sinclair (12) | 0.875 | 0.125 |
| Hampshire (12) | 0.175 | 0.825 |

## Discussion

Basic porcine–human *PXR* gene sequence comparisons revealed that the pig is more similar to the human than other common animal models, including the mouse, rat, rabbit, and dog (Moore et al. 2002). With 85% amino acid sequence identity and 91% similarity, the porcine PXR protein is more equivalent to the human protein than the mouse PXR (O54915), with 77% identity and 86% similarity, or the dog PXR (AAM10632), with 80% identity and 87% similarity. In addition, while there is a size discrepancy between the pig and human PXR peptide, it is due to a 14-aa shorter N-terminal, which is a variable region in even the closest related species. For example, sequence homology between the rhesus monkey and human PXR decreases from 95% overall identity to 86% identity in the first 20 residues of the N-terminal, and this region has yet to be characterized as important to ligand binding or function. While this supports the idea that the pig may be the most appropriate model for *hPXR*, these

comparisons offer only limited information about the nature of the *pPXR*. To provide more insight into the *pPXR*, a profile of splice variants, tissue expression, and genetic polymorphisms was conducted.

The *pPXR* displayed an expression pattern similar to the *hPXR*. Using a single PCR amplification, both human and porcine *PXR* genes were observed to be greatly expressed in the liver, small intestine, and colon (Lamba et al. 2004). Human *PXR* was expressed more abundantly in the stomach, while *pPXR* was expressed more abundantly in the kidney. The human and porcine *PXR* tissue expression patterns become less similar when analyzing tissues with low transcript abundance. In addition to those four tissues with abundant expression, both human and porcine *PXR* transcripts are detected in the adrenal gland and heart. Minor transcript expression exclusive to *hPXR* is detected in the bone marrow and minor expression exclusive to *pPXR* was detected in the thymus, mandibular and mesenchymal lymph nodes, bladder, spleen, testicle, trachea, ovary, and uterus.

SVs of nuclear receptors can alter biological function (Keightley 1998); thus, we sought to identify and characterize *pPXR* SVs. Six novel pig-specific SVs were identified and designated as ssPXR.2–ssPXR.7. Through this study it was determined that previously identified human SVs were unique to the human, although commonalities between the porcine and human *PXR* SVs exist. Most notably, both human and porcine *PXR* SVs were located primarily in the ligand-binding domain. Of the ten *hPRX* transcripts, seven involved a deletion in the ligand-binding domain (Fukuen et al. 2002), and our study demonstrated that five of the six observed pig SVs also involved splicing in the ligand-binding domain.

The *PXR* ligand-binding domain is structured specifically to promiscuously bind to a diverse array of molecules rather than strongly to specific ligands (Watkins et al. 2001). A recent study involving the *hPXR* proposed that SVs add a layer of complexity in PXR activation, allowing changing ratios of SVs present to "fine tune" regulation (Lamba et al. 2004). Although it is unknown what effects *pPXR* SVs have on ligand binding, it could be inferred that these variants act in the same capacity as those studied in the human, because in both cases the variants predict protein alterations within the essential ligand-binding region. More specifically, it could be predicted that SV2, SV3, SV4, SV6, and SV7 have a very different binding profile than wild-type porcine PXR, because up to half of the amino acids that were shown to line the ligand-binding cavity in human PXR (Watkins et al. 2001) are altered in these variants. The truncated peptide and altered ligand-binding domain of these porcine variants are similar to a number of the human PXR variants described previously (Fukuen et al. 2001) and may act in a similar functional capacity. In the future, it will be important to expand examination of the protein structure and function of these variants in more detail.

Overall, the pig and human "wild-type" *PXR* transcripts represent a high degree of similarity. They are also the most abundant, indicating an involvement in common metabolic pathways, including drug responses in both pigs and humans. The species-specific character of splicing in both species suggests that SVs may act as a species-specific mechanism for adaptation to different environmental exogenous compounds encountered by each species.

Similar to the identified SVs, all porcine sequence variation SNPs were located in the ligand-binding domain (exon 5). One SNP (S178L) led to a polar-to nonpolar amino acid change in ligand-binding domain. More specifically, its location corresponded to the α2 helix that is unique to PXR and appears to play an important role in the promiscuous ligand binding of PXR (Watkins et al. 2001). The human PXR contains a serine at this location, with no known polymorphisms. A polar-to nonpolar modification in a region so critical in the functioning of the ligand-binding domain could lead to altered binding abilities. Further investigation, maybe in the form of a reporter assay, must be completed to determine what effects S178L has on ligand binding and CYP3A4 induction.

S178L appears not to be widely distributed and limited to individual pig breeds. The presence of the SNP S178L was screened for in eight diverse breeds of separate origins. All sampled pigs from the Hanford, Yucatan, Duroc, Pietrain, Yorkshire, and Large White breeds were homozygous for cytosine (serine), whereas the Sinclair and Hampshire breeds were heterozygous for cytosine (serine) and thymine (leucine) in this location. Because the *hPXR* contains a guanine (serine) at this point, a pig pharamcogenomic model involving *PXR* might be best developed from the Hanford, Yucatan, Duroc, Pietrain, Yorkshire, or Large White breed.

This study provides a thorough sequence-based (splice variant and SNPs) and tissue expression profile model to support the use of the pig in pharmacogenomic clinical studies; however, there remains much to be investigated in regard to a better understanding of the role of the pig as a model for human metabolism. In the human it has been shown that PXR is not the sole regulator of CYP3A; the constitutive androstane receptor (CAR) also appears

to play a role (Sueyoshi et al. 1999). Although it was indicated that CAR plays a larger role in endogenous chemical metabolism (Huang et al. 2003; Maglich et al. 2004; Saini et al 2004) compared with xenobiotic metabolism in humans, future research should work to more completely characterize the porcine constitutive androstane receptor and explore the interaction between CAR, PXR, and CYP3A activation in pig. While the similarities between murine and human CAR have been analyzed (Moore et al. 2000, 2002), less is known about the porcine CAR. In summary, this characterization of the porcine *PXR* provides a valuable foundation for future research in the development of an additional useful *in vivo* model for metabolic studies.

### Acknowledgments

This work was supported in part by USDA/NRI-CSREES grant AG2001-35205-11698, USDA-ARS AG58-5438-2-313, and Hatch 483-35-314.

### References

1. Bertilsson G, Heidrich J, Svensson K, Asman M, Jendeberg L, et al. (1998) Identification of a human nuclear receptor defines a new signaling pathway for CYP3A induction. Proc Natl Acad Sci U S A 95, 12208–12213
2. Blumberg B, Sabbagh W Jr, Juguilon H, Bolado J Jr, van Meter CM, et al. (1998) SXR, a novel steroid and xenobiotic-sensing nuclear receptor. Genes Dev 12, 3195–3205
3. Fukuen S, Fukuda T, Matsuda H, Sumida A, Yamamoto I, et al. (2002) Identification of the novel splicing variants for the hPXR in human livers. Biochem Biophys Res Commun 298, 433–438
4. Handschin C, Meyer UA (2003) Induction of drug metabolism: the role of nuclear receptors. Pharmacol Rev 55, 649–673
5. Huang W, Zhang J, Chua SS, Qatanani M, Han Y, et al. (2003) Induction of bilirubin clearance by the constitutive androstane receptor (CAR). Proc Natl Acad Sci U S A 100, 4156–4161
6. Hustert E, Zibat A, Presecan-Siedel E, Eiselt R, Mueller R, et al. (2001) Natural protein variants of pregnane X receptor with altered transactivation activity toward CYP3A4. Drug Metab Dispos 29, 1454–1459
7. Kan Z, States D, Gish W (2002) Selecting for functional alternative splices in ESTs. Genome Res 12, 1837–1845
8. Keightley MC (1998) Steroid receptor isoforms: exception or rule? Mol Cell Endocrinol 137, 1–5
9. Kliewer SA, Moore JT, Wade L, Staudinger JL, Watson MA, et al. (1998) An orphan nuclear receptor activated by pregnanes defines a novel steroid signaling pathway. Cell 92, 73–82
10. Koyano S, Kurose K, Saito Y, Ozawa S, Hasegawa R, et al. (2004) Functional characterization of four naturally occurring variants of human pregnane X receptor (PXR): one variant causes dramatic loss of both DNA binding activity and the transactivation of the CYP3A4 promoter/enhancer region. Drug Metab Dispos 32, 149–154
11. Kurose K, Koyano S, Ikeda S, Tohkin M, Hasegawa R, et al. (2005) 5′ diversity of human hepatic PXR (NR1I2) transcripts and identification of the major transcription initiation site. Mol Cell Biochem 273, 79–85
12. Lamba V, Yasuda K, Lamba JK, Assem M, Davila J, et al. (2004) PXR (NR1I2): splice variants in human tissues, including brain, and identification of neurosteroids and nicotine as PXR activators. Toxicol Appl Pharmacol 199, 251–265
13. Langmann T, Moehle C, Mauerer R, Scharl M, Liebisch G, et al. (2004) Loss of detoxification in inflammatory bowel disease: dysregulation of pregnane X receptor target genes. Gastroenterology 127, 26–40
14. Lim YP, Liu CH, Shyu LJ, Huang JD (2005) Functional characterization of a novel polymorphism of pregnane X receptor, Q158K, in Chinese subjects. Pharmacogenet Genomics 15, 337–341
15. Ma X, Shah Y, Cheung C, Guo GL, Feigenbaum L, et al. (2007) The pregnane x receptor gene-humanized mouse: a model for investigating drug-drug interactions mediated by cytochromes P450 3A. Drug Metab Dispos 35, 194–200
16. Maglich JM, Watson M, McMillen PJ, Goodwin B, Willson TM, et al. (2004) The nuclear receptor CAR is a regulator of thyroid hormone metabolism during caloric restriction. J Biol Chem 279, 19832–19838
17. Maurel P (1996) The CYP3A family In: Ioannides C Cytochromes P450: Metabolic and Toxicological Aspects. Boca Raton, FL, CRC Press, 241–270
18. Moore LB, Parks D, Jones S, Bledsoe R, Consler T, et al. (2000) Orphan nuclear receptors constitutive androstane receptor and pregnane X receptor share xenobiotic and steroid ligands. J Biol Chem 275, 15122–15127
19. Moore LB, Maglich JM, McKee DD, Wisely B, Willson TM, et al. (2002) Pregnane X receptor (PXR), constitutive androstane receptor (CAR), and benzoate X receptor (BXR) define three pharmacologically distinct classes of nuclear receptors. Mol Endocrinol 16, 977–986
20. Ostberg T, Bertilsson G, Jendeberg L, Berkenstam A, Uppenberg J (2002) Identification of residues in the PXR ligand binding domain critical for species specific and constitutive activation. Eur J Biochem 269, 4896–4904
21. Pascussi JM, Drocourt L, Fabre JM, Maurel P, Vilarem MJ (2000) Dexamethasone induces pregnane X receptor and retinoid X receptor-alpha expression in human hepatocytes: synergistic increase of CYP3A4 induction

by pregnane X receptor activators. Mol Pharmacol 58, 361–372
22. Saini SP, Sonoda J, Xu L, Toma D, Uppal H, et al. (2004) A novel constitutive androstane receptor-mediated and CYP3A-independent pathway of bile acid detoxification. Mol Pharmacol 65, 292–300
23. Sueyoshi T, Kawamoto T, Zelko I, Honkakoski P, Negishi M (1999) The repressed nuclear receptor CAR responds to phenobarbital in activating the human CYP2B6 gene. J Biol Chem 274, 6043–6046
24. Watkins RE, Wisely GB, Moore LB, Collins JL, Lambert MH, et al. (2001) The human nuclear xenobiotic receptor PXR: structural determinants of directed promiscuity. Science 292, 2329–2333
25. Xie W, Barwick JL, Downes M, Blumberg B, Simon CM, et al. (2000) Humanized xenobiotic response in mice expressing nuclear receptor SXR. Nature 406, 435–439
26. Zhang J, Kuehl P, Green ED, Touchman JW, Watkins PB, et al. (2001) The human pregnane X receptor: genomic structure and identification and functional characterization of natural allelic variants. Pharmacogenetics 11, 555–572